International Journal of Civil Engineering and Technology (IJCIET)
Volume 9, Issue 1, January 2018, pp. 462–471, Article ID: IJCIET_09_01_046
Available online at http://http://www.iaeme.com/ijciet/issues.asp?JType=IJCIET&VType=9&IType=1
ISSN Print: 0976-6308 and ISSN Online: 0976-6316

CALCULATION OF INSTABILITY OF RETAINING WALL OF ROADS INFLUENCED BY GROUNDWATER LEVEL

Huong Thanh Thi Ngo
University of Transport Technology, 54 Trieu Khuc, Thanh Xuan, Ha Noi, Viet Nam

Binh Thai Pham
Department of Geotechnical Engineering, University of Transport Technology,
54 TrieuKhuc, ThanhXuan, Ha Noi, Viet Nam
Department of Civil Engineering, Gujarat Technological University, Nr.Visat Three Roads,
Visat Gandhinagar Highway, Chandkheda, Ahmadabad, Gujarat 382424, India

ABSTRACT

The main aim of this study is to analyze the instability of retaining wall of road during construction of the structure due to the influence of increase of groundwater level. For this, analytic approach and Finite Element Method (FEM) were applied using Midas GTS software. Validation was done by using real observation data. Analysis indicates that the model analysis results are in good agreement with the monitoring data. These results are reliable and can be applied to other project.

Key words: Stability Analysis; Retaining wall; Groundwater Level; Finite Element Method.

Cite this Article: Huong Thanh Thi Ngo and Binh Thai Pham, Calculatıon of Instabılıty of Retaınıng Wall of Roads Influenced by Groundwater Level. *International Journal of Civil Engineering and Technology*, 9(1), 2018, pp. 462-471.
http://www.iaeme.com/IJCIET/issues.asp?JType=IJCIET&VType=9&IType=1

1. INTRODUCTION

Retaining wall is an important geotechnical structure in construction of roads and highways. It has a critical role in keeping stability of foundations and protects talus of slopes. Height of retaining wall in this study was considered varying from from 10m to 20m. These structures usually faces the problems during the construction itself, such as flipping and shear instability and settlement, etc. causing the damage of upper structures including cracked pavement and the formation of sliding bow [1]. The main cause of these problems is due to inappropriate design and construction of embankment and drainage system behind the wall which lead to increase the level of groundwater and thus loads on the retaining wall. In this study, the main objective is to analyze the instability of retaining wall structure during the construction stage influenced by increase of groundwater level and the inappropriate design of drainage system. For this, analytic approach [2] and Finite Element Method (FEM) method [3] were applied

using Midas GTS software [4]. Validation was done by comparing the results with real observation data.

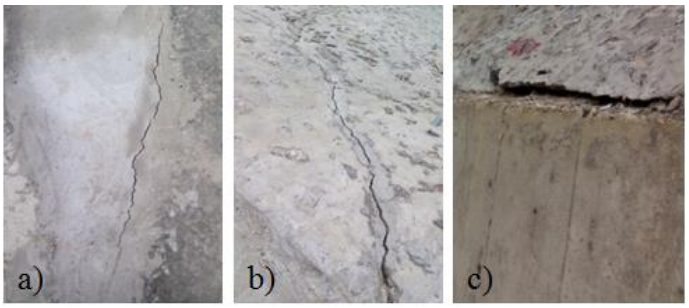

Figure 1 Cracks: (a) cracks on pavements, (b) cracks at the top of slopes, and (c) cracks at the toe of slopes

2. CALCULATION OF INSTABILITY OF RETAINING WALL OF ROAD CONSTRUCTION

In the present study, stability analysis of retaining wall construction for the mountainous roads (category III) has been done. The road is 4 lanes, road width B = 20.5 m . It is designed for the average speed of V=60 km/h. The height of the road embankment varies from 8m to 18.5m. In this study two types of retaining walls were designed: (1) reinforced concrete wall with L-shaped cross section, height H_1 = 10m, length 32m, divided into units, (2) gravity concrete wall with height H_2 = 4.0 m - 8.0 m, length 40m, divided into 6 units. The total length of the retaining wall is 72m. Foundation of retaining wall is shallow, the peak of wall has slope height of 8m, slope coefficient m = 1.5. During the finishing phase, the wall was observed moved downstream. Cracks on the slope and pavement were also observed (Figure 1).

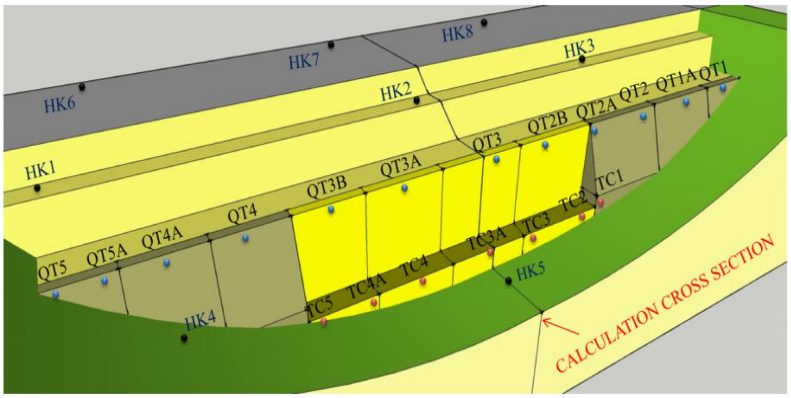

Figure 2 Diagram of geological exploratory holes and monitoring points of displacement of retaining wall

Because of the above reasons, further exploration was carried out in the area by dredging downhill slope and geological exploratory drills. Drainage design and functioning of drainage of the walls were rechecked. Monitoring points at the top and toe of the walls were marked to measure displacement (Figure 2).

2.1. Analysis of the Effect of Groundwater in the Stability of the Retaining Wall

While drilling HK2 at a depth of -3.5 m (Point A), a dehydration soil pit was encountered at the junction between the embankment and the original soil - clay mixed with earthen meshes. The thickness of the dehydrated soil layer is about 2.0 m. This layer is having effect of conducting water from upstream to downstream. Boring hole HK7 on the positive side has

encountered dehydrated weathered rock at a depth of -0.5 m (Point D). According to the monitoring data, on June 9th, 2017, water levels in HK1 and HK2 rose +1.5 m to +0.00 m (Point B). On June 14th, 2018, the groundwater level in the wall continued to rise due to no-stop rainfall. Direct observation data indicate that the water was flowing into the nozzles from the top of the hole from -1.5 m to -2.0 m (Point C).

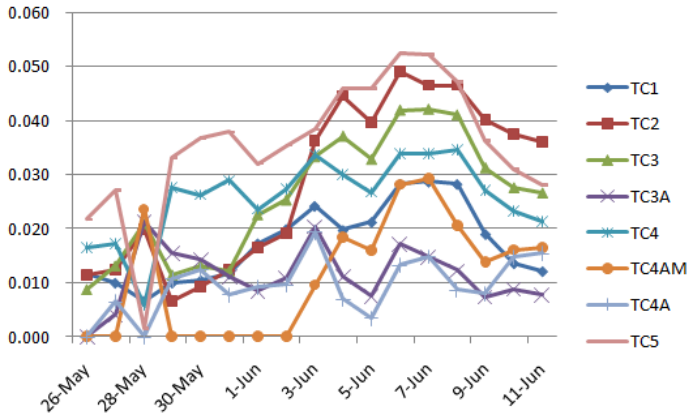

Figure 3 Displacement of wall foundation (m)

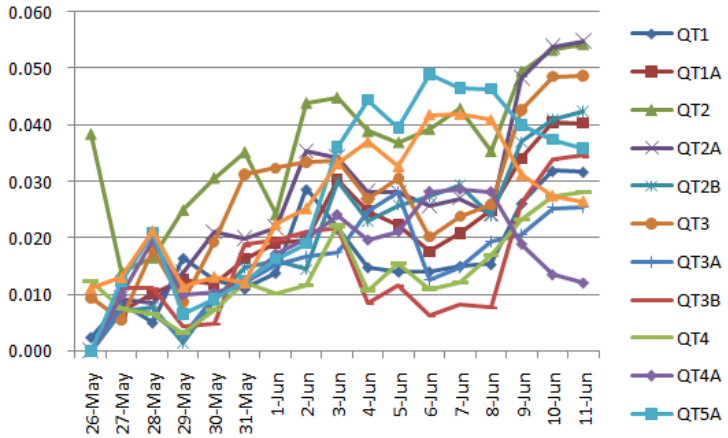

Figure 4 Displacement of peak of wall (m)

Observation of boring hole for checking the drainage on the back of the wall shows no water was draining out from all inspection holes. During rainy days, the water level was at a height of -2.0 m compared with the top of the wall. However, no water is draining out through the drainage holes below the wall. It can be concluded that the back drainage system was clogged which increased the pressure on the wall and reduced the shear strength of the embankment.

2.2. Analysis of Displacement Data of Retaining Wall

Displacement of wall foundation and peak observed from May 26th to June 11st, 2017 is shown in Figure 3 & 4. Analysis results show that the entire retaining wall is transversely displaced. The peak of wall has the highest displacement with the third unit (H = 8mm) from left to right (QT2 and QT2A) is 55mm. The peak of wall has a second ranked displacement (H = 4mm) from left to right (AT5 and AT5A) is 50mm. The highest displacement of the toe of wall is placed at outside units (TC5 and TC2) is about 50mm.

To analyze accurately the displacement law of the retaining wall, we converted the chart of displacement of peak and and foundation of wall to the parallel curves (Figure 5). These

curves do not reflect accurately the actual displacement but allow the viewer to see the overall transformation law.

Figure 5 show that it is possible to divide the instability of reinforced concrete retaining wall into three stages as follows:

Phase 1 (from May 26th to June 3rd, 2017): Displacement of the top and the foundation of the wall increased gradually, the average displacement of both the top and the foundation was was 20.0 mm. However, the rule of increase of the displacement of the top of the wall is more regular than the foundation. In this stage, the whole wall is pushed downstream, the wall has a flat instability.

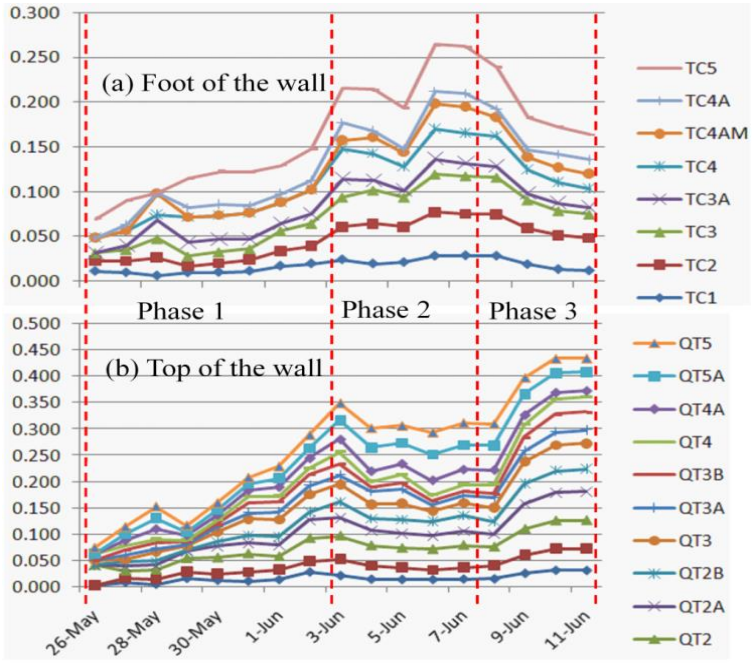

Figure 5 The calibrated displacement according to rule

Phase 2 (from June 3rd to 8th 2017): Displacement of the top of the wall abruptly decreased by about 5.0 mm then almost remained unchanged. But overall, the bottom of the wall continueed to move; especially the locations TC1, TC2, TC3, TC4A and TC5 have a large increasing amplitude of about 16.0 mm. The wall has a rotating instability with the center of rotation is in the top of the wall, the foot of the wall was pushed downstream. This phenomenon is caused by the excavation of the slope at the top of the wall which makes the movement of the top of the wall, but it has not affected to the displacement of the bottom of the wall. Thus the displacement continued to rise. In this stage, the sliding under the foundation wall was noticed.

Phase 3 (from June 8th to June 11th 2017: On June 9th, the displacement of the top of the wall started which increased suddenly to about 10.0 mm and then increased up to 15.0 mm by June 10th. On June 8th, the displacement tends to shift back upstream about 5.0mm, until June 10th the reversal is about 18.0mm, particularly at measuring points TC3 and TC5 that is 20.0mm and 25.0mm, respectively. Instability of the wall turned around a certain point at about 1/3 of the wall height. This phenomenon slowly down from June 10th onward. Instability of the wall in this phase is caused by heavy rainfall on June 8th and June 9th due to increase of groundwater.

2.3. Analysis and Calculation of Instability of the Wall

Using the geotechnical software named Midas GTS, the seepage stability and overall sliding of the wall were calculated. Midas GTS is a system of advanced geotechnical and road structure software. It was developed on the basis of the experience of the FEM and geometric technology [4].

2.3.1. Seepage Stability

Determination of saturation line in the ground (the water pressure on the back of the wall) using the calculating model of seepage in Midas GTS software with equations as follow:

In case of stable infiltration:

$$\frac{\partial}{\partial x}\left(k_x \frac{\partial H}{\partial x}\right)+\frac{\partial}{\partial y}\left(k_y \frac{\partial H}{\partial y}\right)+\frac{\partial}{\partial z}\left(k_z \frac{\partial H}{\partial z}\right)+Q=\frac{\partial \Theta}{\partial t} \quad (1)$$

In case of unstable infiltration:

$$\frac{\partial}{\partial x}\left(k_x \frac{\partial H}{\partial x}\right)+\frac{\partial}{\partial y}\left(k_y \frac{\partial H}{\partial y}\right)+\frac{\partial}{\partial z}\left(k_z \frac{\partial H}{\partial z}\right)+Q=\left(\beta S_s+\frac{\partial \Theta}{\partial H}\right)\frac{\partial H}{\partial t} \quad (2)$$

where H is total water column (m), k_x is the coefficient of permeability in the direction x, (m/s), k_y is the coefficient of permeability in the direction y (m/s), k_z is the coefficient of permeability in the direction z (m/s),Q is flow in a unit of volume per unit of time (m^3/s),Θ is water content, t is time (s),β is the coefficient of water storage, S_s is water storage capacity.2.3.2 Overall sliding stability

Method which is selected for calculation of stability of the retaining wall is the method of reduction of φ, c (Figure 6). The main principle of this method is to reduce gradually the shear resistance of embanking materials to the point of assumption at which the sliding instability occurred. The maximum ratio of shear resistance reduction at that time is considered as the minimum safety factor as following formula (3).

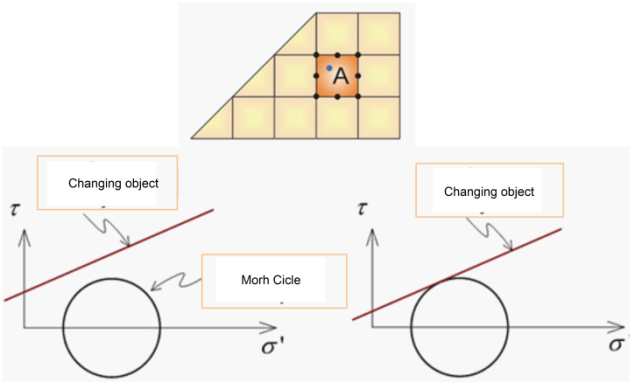

Figure 6 Reduction mechanismφ, c

The coefficient of slipping safety is determined on the basis of the shear failure as follows:

$$F_s=\frac{\tau}{\tau_f} \quad (3)$$

whereτ is the shear resistance of materials, $\tau = c + \sigma_n \tan\phi$, (kN/m^2), τ_f is the shear resistance of shear plane, $\tau_f = c_f + \sigma_n \tan\phi_f$ (kN/m^2).

$$c_f = \frac{c}{SRF} \tag{4}$$

$$\phi_f = \tan^{-1}\left(\frac{\tan\phi}{SRF}\right) \tag{5}$$

where SRF is the intensity reduction factor, which depends on the number of iterations to converge and the unbalance index specified by the user.

3. A CASE STUDY

3.1. Calculation Models

Based on the real situation, geological documents and the groundwater level behind the wall, etc. This paper analyzes several specific cases to find the failure form of the wall. The cases for calucaltion are shown in Table 1 and Figure 7.

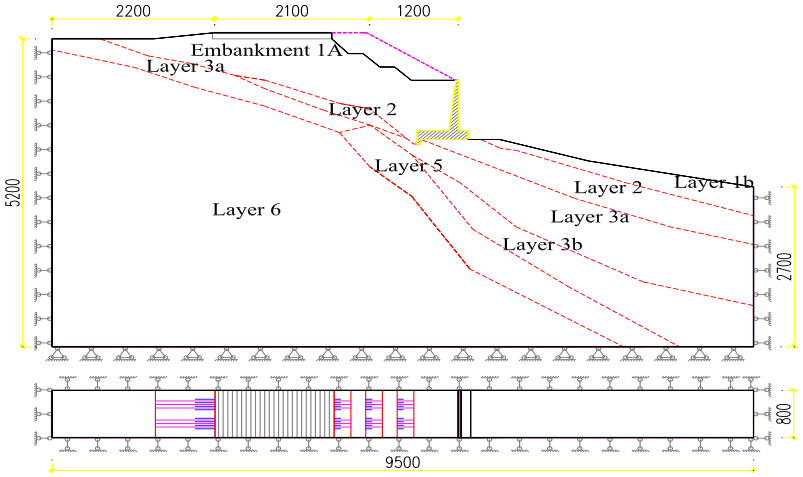

Figure 7 The diagram for calculation

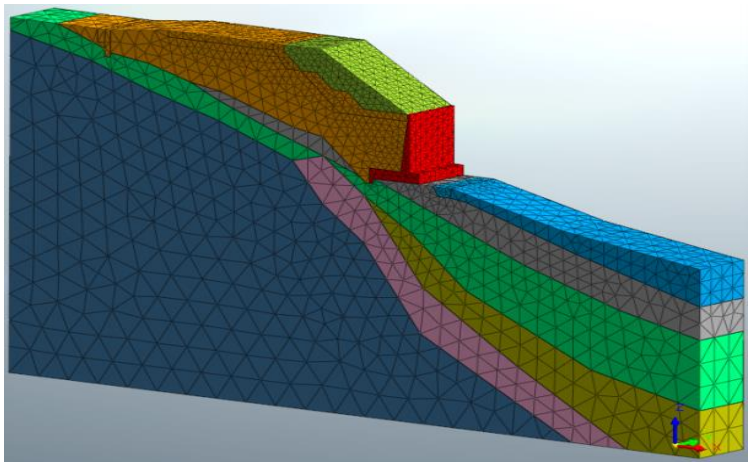

Figure 8 The model of the retaining wall

3.2. Construction of the Models

Constructing the model for calculation of one unit of 8.0m length. Using the model of Mohr-Coulumb in Midas GTS software to calculate. The dimention of the model is 8.0 width, 95m length and 52.0m height. The wall has the L shape with the hight of 8.5m, the height of the foot of the wall is 1.5m (Figure 8).

Table 1 The caluclation cases

	Case 1	**Case 2**	**Case 3**	**Case 4**
Case study	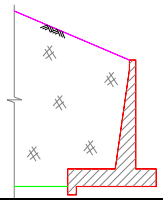	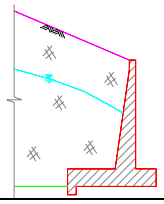	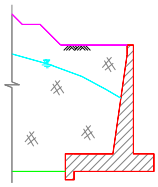	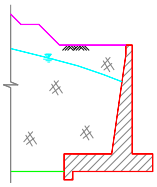
Description	No groundwater leval	Groundwater leveral is rose by rainfall (the water inside the ground, thus it cannot drain due to the filter system is stuck)	Lowering the slope, the groundwater level is equivalent to the water level of TH2).	Lowering the slope, the groundwater level is increased compared to the water level of TH2 due to the increase of rainfall).

The loads for calculation include self-loads, vehicle-loads, water pressure. Boundary conditions: The boundary X is fixed in X direction, the boundary Y is fixed in Y direction, the boundary Z is in the bottom of the model which is fixed in X, Y, Z, and the upper side of the model has no boundary condition. Main steps for calculation: (1) calculate the stress caused by the soil itself, (2) calculate the stress due to the retaining wall load, and (3) calculate the wall stability.

Mechanical properties of soil of the foundation and embankment were determined and collected from the experimental documents as shown in Table 2.

Table 2 Mechanical properties of soil of the foundation

Layers	$\gamma_{naturak}$ **(kN/m^3)**	$\gamma_{saturated}$ **(kN/m^3)**	ν	E **(kN/m^2)**	K **m/s**	c **(kN/m^2)**	φ **(°)**
Embankment	19.3	20.3	0,3	12000	$1.4x10^{-7}$	23.4	17.3
Layer 2	19.7	20.7	0,3	12500	$1.6x10^{-6}$	23.3	13.6
Layer 3a	21.8	22.8	0,3	23000	$1.5x10^{-7}$	30.8	19.0
Layer 3b	21.0	22.0	0,3	18000	$1.8x10^{-7}$	40.1	20.6
Layer 4	20.7	21.7	0,3	20000	$5.4x10^{-7}$	23.8	18.6
Layer 5	21.4	22.4	0,3	21000	$1.2x10^{-8}$	25.3	19.0

Note: Embankment – Graveled clay, hard to semi-hard plastic, SPT = 27; Layer 2: mixed clay, blue-gray, hard plastic, SPT = 17; Layer 3a: mixed clay, sepia, hard plastic to semi-hard, SPT = 18; Layer 3b: mixed clay, sepia, hard to very hard, SPT = 79; Layer 4: mixed clay, gold-gray, hard plastic to semi-hard, SPT = 48; Layer 5: mixed clay, black-gray, semi-hard to hard, SPT = 16.

3.3. Results and Analysis

3.3.1. Seepage Stability

The permeability calculation for case 1 shows that the water flow through the contiguous region between the new embankment and the ground, the saturated line (BH1) tends to the foot of the retaining wall(Figure 9). The calculated results are consistent with the monitoring results of point A (HK2) and point D (HK7). In this case, it is possible to ignore the effect of groundwater in calculating the stability of the retaining wall.

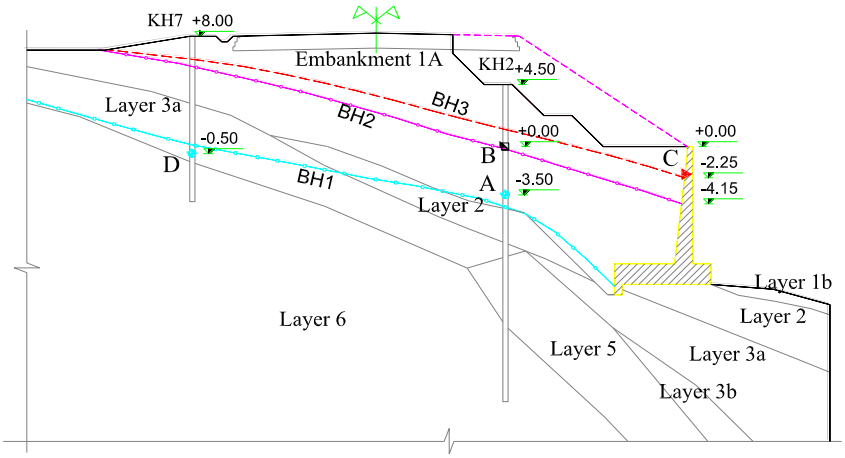

Figure 9 Simulation of the retaining wall

In the case we consider the rain for calculation, the drainage filter behind the retaining wall is damaged, we obtained the saturation line (BH2). The calculated water height compared to the foot of the wall is 5.85 m. The results are consistent with the monitoring results of point B (HK2).

In the cases where slope is lowered, and the rain is also increased, the drainage filter behind the retaining wall was damaged, we obtained the saturation line (BH3). The height of the water column calculated against the foot of the wall is 7.75 m. The results of the calculation are consistent with the monitoring results of point C (HK2) located beyond the retaining wall.

The calculation results of the saturation line beyond the retaining wall of the cases are consistent with the fact that they have a great influence on the stability of the wall. These calculations values will be the inputed in the analysis of the stabilization of the wall. The case 1 uses saturated line 1 (BH1); the case 2 uses saturation line 2 (BH2); the cases 3 and uses saturation line 1 (BH3).

3.3.2. Overall Sliding Stability

The overall sliding stability calculation was carried out by analytical method and the FEM (Midas GTS). The calculated results are shown in Table 3 and Table 4. The calculation results of case 1 with the saturation line of BH1 using the analytic method and the FEM are safe. However, the displacement of the top of the wall is very large 215.8 mm; thus, the wall is at risk of instability.

In the case 2, the groundwater level rise with the saturation line of BH2. The results of analytic method show the flippong instability of the wall with K = 0.84. According to the FEM, the safety factor is K = 1.15 which is less than the allowed value. The displacement of the top of the wall is very large 324.7 mm; the wall is at risk of rotated-sliding instability. The calculated results are consistent with actual observations.

Table 3 Calculation by analytical method

Computational requirements	Case 1	Case 2	Case 3	Case 4
Bearing capacity of foundation	Accepted	Accepted	Accepted	Accepted
Flipping stability factor	Accepted: K=2.65	Accepted: K=1.77	Accepted: K=1.85	Accepted: K=1.81
Sliding stability factor	Accepted: K=1.23	Not accepted: K=0,84	Not accepted: K=0,93	Not accepted: K=0,89

Note: Flipping stability coefficient allowed is1.5; Sliding stability coefficient allowed is 1.20 [3].

Table 4 Stability coefficient (K) and the maximum displacement (Z) using the FEM method

Case 1	Case 2	Case 3	Case 4
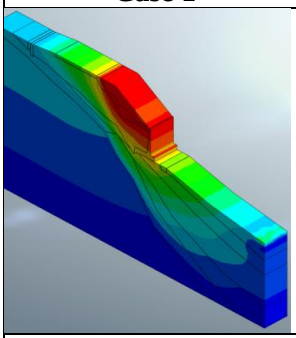	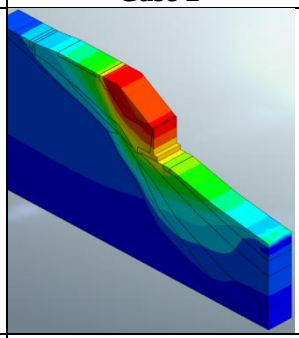	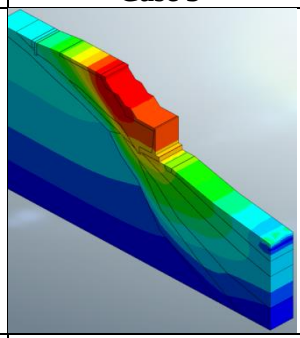	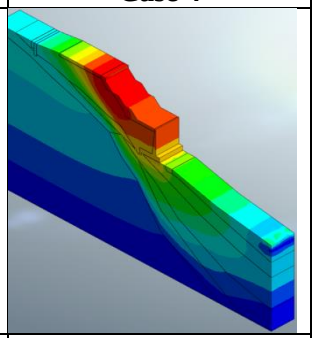
K = 1.20, Z = 215.8 mm.	K = 1.15, Z = 324.7 mm.	K = 1.33, Z = 44.2 mm.	K = 1.27, Z = 48.5 mm.

Note: Coefficient of stabilityallowed is1.25 [4].

In the case 3, the groundwater level rise with the saturation line of BH2. The results of analytic method show the flippong instability of the wall with K = 0.93. According to the FEM, the safety factor is K = 1.33 which is slightly higher than the allowable value. The displacement of the top of the wall is 44.2 mm indicating the instability of rotated-sliding. The calculated results are consistent with actual observations.

In the case 4, the groundwater level rises above the level of the case 2 due to the increased rainfall with the saturation line of BH3. The results of analytic method show the flipping instability of the wall with K = 0.89. According to the FEM, the safety factor is K = 1.27 which is approximately equal to the allowed value (Figure 10). The displacement at the top of the wall is 48.8 mm, at the foot wall is 25.3 mm indicating the instability of rotated-sliding. The calculated results are in accordance with the actual observation results such as at the top of the wall is 49.0 mm (QT3), at the foot of the wall is 21.0 mm (TC3A).

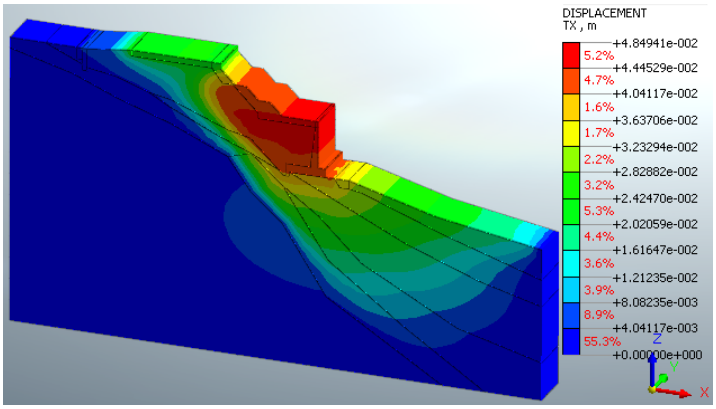

Figure 10 The calculation results of displacement of the case 4

In all cases FEM show occurrence of shallow slides. In the case of continuing movement/ displacement up to top of the wall, it is necessary to take measures to reinforce and prevent the slipping of the retaining wall.

4. CONCLUSIONS

In this study, analysis of the instability of retaining wall under construction for the road was done to assess the influence of increase in groundwater level behind wall. For this analytic approach and the FEM method were used in Midas GTS software. Validation was done by comparing the results with real observation data.

Model analysis results show that they are in good agreement with the monitoring data. Units of retaining wall has a similar instability rule that ranges from flat shear instability to reversing instability of wall toe to the upstream, and eventually flipping the wall to the downstream. The analysis results are reliable and can be applied to other project.

In the future work, we focus on the analysis of overall stability of retaining wall by 3D model using Midas GTS software with the length of 72m to find the instability units of the wall compared with available monitoring results.

REFERENCES

[1] Braja M. Das, Foundation Engineering, China machine press, 2016.

[2] 22TCN 272-05, Standard of bridge design, 2005.

[3] TCVN 9152: 2012, Irrigation Works - Procedure of design of the retaining wall of irrigation works, 2012.

[4] Midas Geotechnical and Tunnel Analysis System, *MIDAS Information Technology Co., Ltd.*,.,2014.

[5] Ify L. Nwaogazie, Adekunle O. David and Oghenefejiri Bovwe, Computer Simulator (RETFLO) For Retaining Wall Flood Bank Protection Design. International Journal of Civil Engineering and Technology, 7(4), 2016, pp.246–268.

[6] Abdul-Hassan K. Al-Shukur and Ayaat Majid Abbas Al -Rammahi, Optimum Design of Semi-Gravity Retaining Wall Subjected to Static and Seismic Loads. International Journal of Civil Engineering and Technology, 8(1), 2017, pp. 873–881.

[7] Sandeep K. Chouksey and Abhishek Fale, Reliability Analysis of Counterfort Retaining Wall, International Journal of Civil Engineering and Technology, 8(7), 2017, pp. 1058–1073